Design, prototyping and beam testing of an interaction point feedback system for the International Linear Collider

R. J. Apsimon,* D. R. Bett,† N. Blaskovic Kraljevic,‡ R. M. Bodenstein, T. Bromwich, P. N. Burrows, G. B. Christian, B. D. Constance, M. R. Davis, C. Perry, and R. Ramjiawan
John Adams Institute for Accelerator Science at University of Oxford, Denys Wilkinson Building, Keble Road, Oxford OX1 3RH, United Kingdom
(Dated: March 16, 2017)

Abstract.

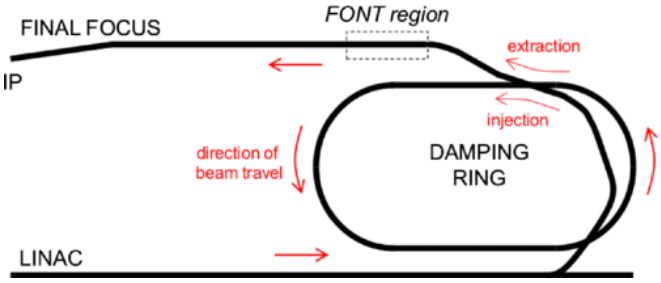

FIG. 1: Layout of the ATF, showing the locations of the ATF2 extraction line and the FONT system.

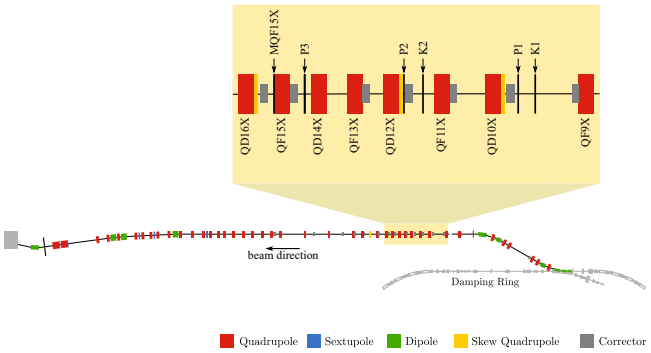

FIG. 2: Layout of the ATF extraction and final focus lines [7], indicating the location of the stripline BPMs (P1, P2, P3 and MQF15X) and kickers (K1 and K2) used by the FONT system. Quadrupole magnets ('Q') are shown.

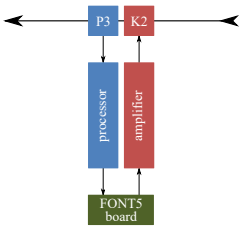

FIG. 3: Block diagram of the feedback system.

I. INTRODUCTION

II. EXPERIMENTAL SETUP

The feedback system described in this paper has been developed by the Feedback on Nanosecond Timescales (FONT) group [1] and has been installed, commissioned and tested at the Accelerator Test Facility (ATF) [2] at KEK. The ATF (Fig. 1) is a test accelerator for the production of very low emittance electron beams as required for the future generation of ILC-like linear electron accelerators. In 2008, as part of the ATF2 project [3], the accelerator was upgraded, with the existing extraction line being replaced with one leading to an energy-scaled version of the compact focusing optics designed for the ILC [4]. The goals of the ATF2 collaboration [5] are, firstly, to achieve a 37 nm vertical spot size at the final focal point and, secondly, to stabilise it to the nanometer level.

As part of the ATF beam stabilisation goal, the FONT group has developed a beam position stabilisation system ('FONT5') [6] deployed close to the start of the ATF extraction line (Fig. 1). The full feedback system has been designed to stabilise both the beam position and angle, in the vertical plane, such that the correction propagates into the ATF final focus line. For this purpose, the feedback system comprises the stripline beam position monitors P2 and P3, and the kickers K1 and K2, with their layout shown in Fig. 2. Furthermore, in the context of the demonstration of an ILC-like IP position feedback system, the FONT5 system has been operated in 'single-loop' mode using P3 to measure and K2 to correct, as shown in Fig. 3. The hardware components in the feedback loop are presented below.

A. Stripline BPM and processor

The FONT stripline BPMs, with their associated analogue processors, have been developed specifically for high resolution and low latency. Each stripline BPM consists of four 12 cm strips, arranged as two orthogonal diametrically opposed pairs separated by 23.9 mm

* Present address: Cockcroft Institute, University of Lancaster, UK.
† Present address: CERN, Geneva, Switzerland.
‡ neven.blaskovickraljevic@physics.ox.ac.uk

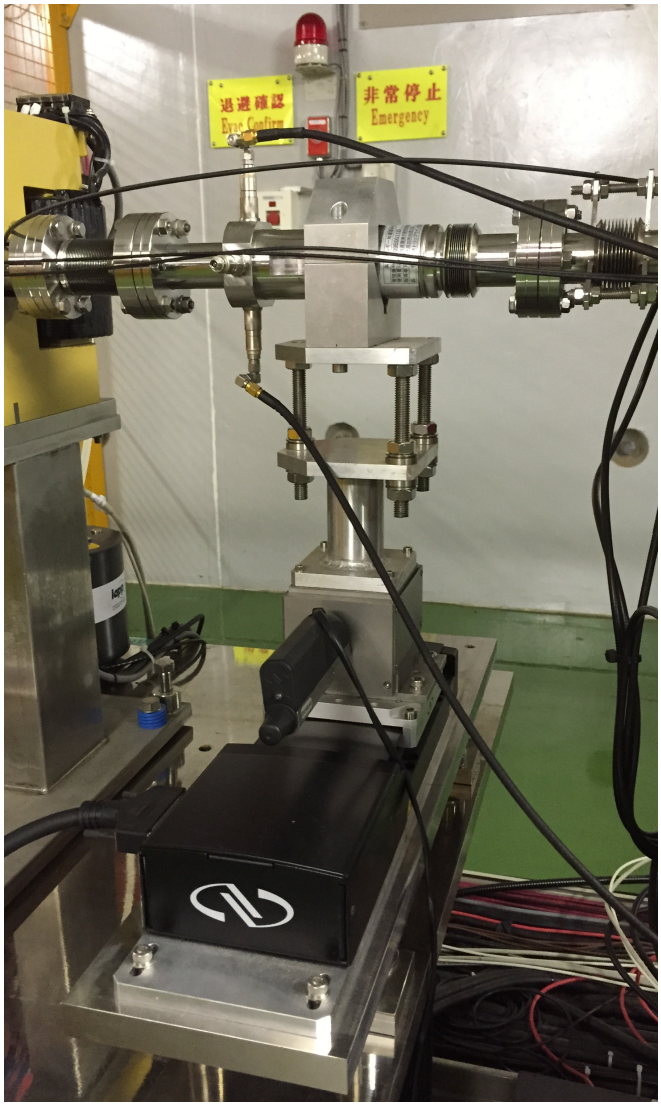

FIG. 4: Photograph of the stripline BPM P3 and its mover in the ATF beamline.

[8]. BPMs P1, P2 and P3 are each mounted on a mover (Fig. 4) [9] that can translate the BPM vertically and horizontally in the plane perpendicular to the beam, allowing the beam to be centered within each BPM aperture; a further stripline BPM (MQF15X) is located 0.76 m downstream of P3.

A single BPM processor can be used to process the beam position data in either the horizontal or vertical plane; from here on only the vertical plane is considered. The stripline BPM processors employ a 'difference-over-sum' signal processing technique as follows. The signals from the top and bottom strips are added using a resistive coupler, and subtracted using a 180° hybrid. An external, continuous, machine-derived local oscillator (LO) is used to down-mix the sum and difference signals to produce the baseband signals V_Σ and V_Δ, respectively. These signals can then be digitised, and the beam position calculated as being proportional to $\frac{V_\Delta}{V_\Sigma}$.

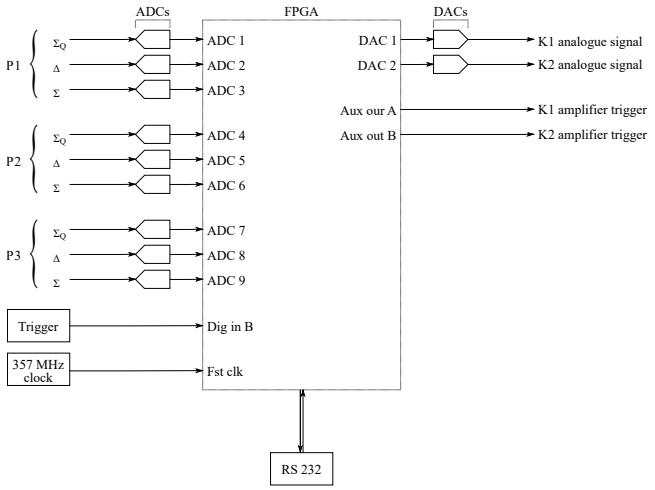

FIG. 5: Schematic of the FONT5A board.

The stripline BPM system has a demonstrated position resolution of 291 ± 10 nm at a bunch charge of ~ 1 nC, with a linear dynamic range of ± 500 μm [8]. The processor latency has been measured to be 15.6 ± 0.1 ns [8].

B. FONT5A digital board

The stripline BPM outputs are digitised in the FONT5A digital feedback board (Fig. 5). The board consists of a Xilinx Virex-5 field programmable gate array (FPGA) [10], nine TexasInstruments ADS5474 14-bit analogue-to-digital convertors (ADCs) [11] and two Analog Devices AD9744 14-bit digital-to-analogue convertors (DACs) [12] used to drive the kickers. An external trigger, preceding the extraction of the bunches from the ATF damping ring, is used to ensure that the data acquisition is synchronised to the bunch arrival time. Each ADC is clocked with a 357 MHz signal synchronised with the ATF damping ring RF. Data is sent serially from the board via a UART over RS232. In addition to sampling the analogue waveforms from the BPM processors, the FONT5A board also provides the required drive and trigger signals to the kickers.

For a given train of bunches, the FONT5A board measures the position of the first bunch and attempts to zero the position of subsequent bunches. If y_n is the uncorrected position of the n^{th} bunch, and Y_n is the position of the n^{th} bunch with the feedback on, the formula for bunch-to-bunch feedback is:

$$Y_n = y_n - y_{n-1} - \delta_n, \tag{1}$$

where δ_n is a constant offset that can be applied to the n^{th} bunch. As it is the corrected position that is measured for the second and subsequent bunches, and not

the position they would have in the absence of the feedback correction, the system uses the corrected positions as follows:

$$Y_n = y_n - \sum_{i=1}^{n-1} Y_i - \delta_n, \tag{2}$$

where $Y_1 = y_1$. The correction applied to previous bunches are added to the delay loop in the FPGA firmware, constituting the memory of the total correction performed on the train of bunches.

The DAC issued to the K2 amplifier by the FONT5A board, V_{DAC}, is given by:

$$V_{\mathrm{DAC}} = G\frac{V_\Delta}{V_\Sigma} + D + \delta, \tag{3}$$

where G is the pre-loaded feedback gain, V_Σ and V_Δ are the digitised sum and difference signals from the P3 processor, D is the value stored in the delay loop and δ is the constant DAC offset applied to the given bunch. The gain can be calculated from the gradient H of the measured $\frac{V_\Delta}{V_\Sigma}$ versus the set V_{DAC} by the relationship:

$$G = -\frac{V_{\mathrm{DAC}}}{(\frac{V_\Delta}{V_\Sigma})} = -\frac{1}{H} \tag{4}$$

where the minus sign originates from the requirement that the feedback subtracts the offset measured.

C. Kicker and amplifier

The kickers (Fig. 6), provided by the SLAC laboratory, each consist of two parallel conducting strips placed along the top and bottom of the beampipe. Driven with input signals from one end, the kickers can deflect the beam in the y direction. The DAC analogue outputs from the FONT5A board are passed through a custom-built amplifier for each kicker, delivering a high current with a rise-time of a few tens of nanoseconds. The required amplifier was developed and manufactured for this purpose by TMD technologies [13] and can provide ±30 A of drive current with a rise-time of 35 ns from the time of the input signal to reach 90% of peak output. The output pulse length is specified to be up to 10 μs. The TMD amplifiers need to be triggered in advance of the bunch arrival; these triggers are generated by the FONT5A board (Fig. 5).

III. SYSTEM PERFORMANCE

A. System latency

The latency of the system was measured using a special mode of the FPGA firmware, where the FONT5 board timing remains unchanged but the DAC output is replaced by a constant setting, providing a static kick to the beam one latency period after the measurement of the first bunch. By varying the bunch strobe set for the first bunch relative to that of the second bunch, the effective bunch separation can be varied, and the kick applied to the second bunch can be studied. Data was taken with interleaved kicked and unkicked beam to mitigate against beam drift, and averaged at each setting to remove the effect of beam jitter on the measurement. Fig. 7 shows the average difference between kicked and unkicked position versus bunch spacing, with a cubic smoothing spline fit. The system latency is defined as the point at which 90% of the full kick is seen, corresponding to a latency of 148 ns for the data in Fig. 7.

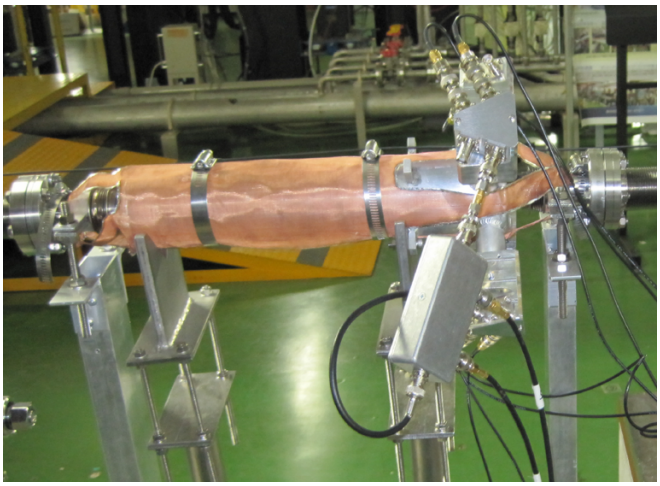

FIG. 6: Photograph of the kicker K2 in the ATF beamline.

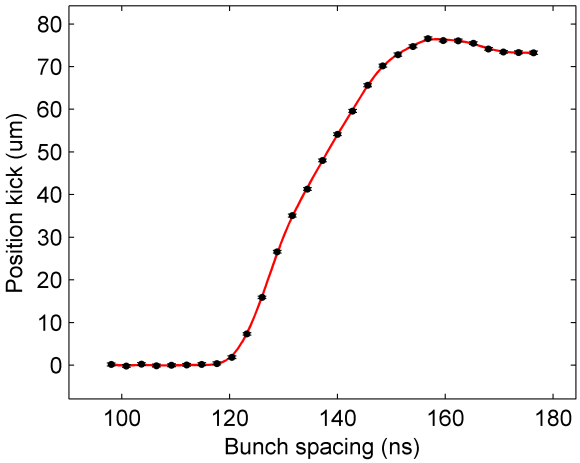

FIG. 7: Average difference between kicked and unkicked positions for bunch 2 at P3 versus bunch spacing. Standard errors are given; the line is a cubic smoothing spline fit.

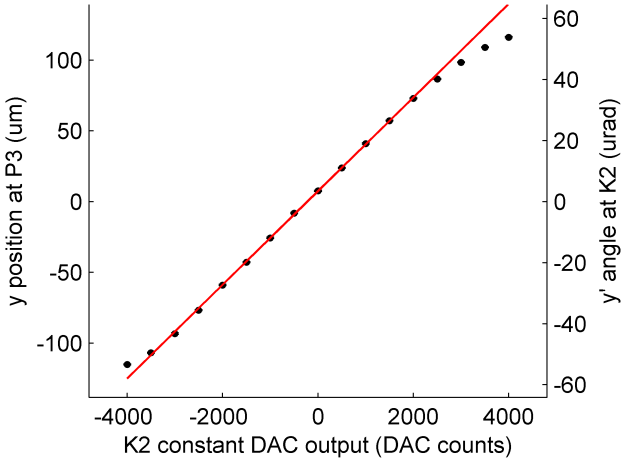

FIG. 8: Vertical position at P3 (left axis) versus constant kick applied at K2. The right axis shows the corresponding y' kick applied at K2. Standard errors are given; the line is a linear χ^2 fit to the central nine data points.

B. Kicker linearity and range

The K2 kicker performance was tested by scanning the DAC output sent to the kicker and measuring the beam displacement at P3 (Fig. 8). The angular kick y'_{K2} imparted to the beam by K2 can be reconstructed from the measured kick y_{P3} at P3 using element M_{34} of the 6×6 linear transfer matrix M from K2 to P3 (extracted from the ATF MAD model [14]):

$$y_{\mathrm{P3}} = M_{34} y'_{\mathrm{K2}}. \tag{5}$$

A linear kicker response is observed in Fig. 8 over a dynamic range of ± 60 μm at P3, corresponding to a kick dynamic range of $\sim \pm 30$ μrad at K2. The size of the kick scales to $\sim \pm 70$ nrad at the full 500 GeV ILC beam energy, which exceeds the requirements discussed in Sec. I.

C. Feedback results

The ATF was configured with three bunches per train and a bunch separation of 154 ns. The beam was centered in both P3 and MQF15X by using an upstream corrector magnet; the beam was further centred in P3 by using the BPM mover. The feedback was operated in interleaved mode, where alternate trains are operated with feedback off and on. The data where the feedback is off are used to characterise the undisturbed beam and to identify drifts in the incoming beam conditions.

The feedback performance (Fig. 9) is monitored at P3. As expected, the first bunch is not affected by the feedback as this bunch is only measured. The second and third bunches show the effect of the feedback: the bunches are centred on zero and the spread of positions is reduced.

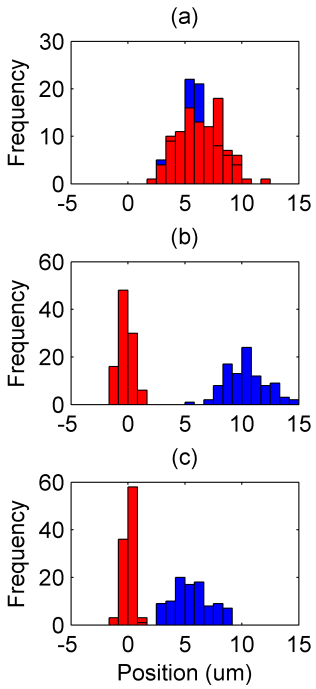

FIG. 9: Distributions of positions with feedback off (blue) and feedback on (red) measured at P3 for (a) the first, (b) the second, and (c) the third bunches.

TABLE I: Mean position and jitter with feedback off and on for bunches 1, 2 and 3 at P3. Standard errors on the mean and jitter are given.

	Mean position (μm)		Position jitter (μm)	
Bunch	Feedback off	Feedback on	Feedback off	Feedback on
1	5.97 ± 0.16	6.37 ± 0.19	1.61 ± 0.12	1.93 ± 0.14
2	10.39 ± 0.17	-0.25 ± 0.06	1.65 ± 0.12	0.60 ± 0.04
3	5.58 ± 0.17	0.04 ± 0.05	1.63 ± 0.12	0.45 ± 0.03

The mean position and jitter (one standard deviation of the spread of positions) at P3 are quoted in Table I. The feedback acts to reduce the incoming beam jitter from ~ 1.6 μm to 600 nm and below. The uncorrected bunch train is observed to have a static bunch-to-bunch position offset of ~ 5 μm; the feedback then centres the mean position of both bunches two and three to within 0.25 μm of P3's electrical centre through the use of the constant offset δ_n (Eq. 1).

A high incoming bunch-to-bunch position correlation, in excess of 94% for this data set (Table II), is central to obtaining the reduction in position jitter reported here. The feedback then acts to remove the position components that are correlated between the bunches, bring the correlation down to $\sim 0\%$.

The expected feedback performance can be predicted

TABLE II: Bunch-to-bunch correlation with feedback off and on at P3. Standard errors are given.

	Correlation (%)	
	Feedback off	Feedback on
Bunch 1 to bunch 2	$+94 \pm 1$	-11 ± 10
Bunch 2 to bunch 3	$+96 \pm 1$	-28 ± 9

for the case of a perfect on-board feedback calculation and a linear kicker response by taking the standard deviation of the terms in the feedback algorithm in Eq. 1:

$$\sigma_{Y_n}^2 = \sigma_{y_n}^2 + \sigma_{y_{n-1}}^2 - 2\sigma_{y_n}\sigma_{y_{n-1}}\rho_{y_n y_{n-1}}, \qquad (6)$$

where σ_{Y_n}, σ_{y_n} and $\sigma_{y_{n-1}}$ are the standard deviations (position jitters) of Y_n, y_n and y_{n-1} position distributions and $\rho_{y_n y_{n-1}}$ is the correlation of y_n to y_{n-1}. Substituting the data with feedback off from Tables I and II into Eq. 6 yields predicted jitters of $\sigma_{Y_2} = 0.58$ μm and $\sigma_{Y_3} = 0.45$ μm for bunches two and three, respectively, at P3 with feedback on. These values agree closely with the measured jitters of 0.60 ± 0.04 μm and 0.45 ± 0.03 μm for bunches two and three, respectively, indicating that the feedback and kicker system are functioning as expected.

Fig. 10 shows the measured feedback performance at MQF15X. The level of jitter reduction is not as pronounced as at P3, as the feedback system is designed to stabilise the beam at the feedback BPM. However, the jitter measured at MQF15X is found to agree well with that expected from propagating the measured beam at BPMs P2 and P3 (Fig. 2) using linear transfer matrices extracted from the ATF MAD model [14], as shown in Fig. 10.

The orbit of the beam arriving to P3 was swept vertically through a range of over 100 μm by varying the setting of the corrector magnet ZV6X, located upstream of K2, in order to assess the feedback operation over a wide dynamic range. The results with feedback off and on, in Fig. 11, show that the position of the second bunch is centered and the spread of positions is reduced consistently over the full range of the scan. Successful stabilisation of the third bunch has allowed the mean position of the train to be corrected to zero for the bunches following the first bunch, as shown in Fig. 12.

Two vertical steering magnets were used to enhance the natural beam jitter entering the feedback system, with the magnets applying a random kick conforming to a pre-defined distribution and updating the kick at the train repetition frequency. The feedback is observed to continue successfully centering and stabilising the beam, even when the full spread of uncorrected positions exceeds ± 100 μm, as shown in Fig. 13.

IV. CONCLUSIONS

[1] `http://www-pnp.physics.ox.ac.uk/~font/index.html`.

[2] F. Hinode, S. Kawabata, H. Matsumoto, K. Oide, K. Takata, S. Takeda, and J. Urawaka, *Accelerator Test Facility: Design and study report*, Tech. Rep. 95-4 (KEK Technical Report, 1995).

[3] B. Grishanov *et al.* (ATF2 Collaboration), *ATF2 Proposal*, Tech. Rep. 2005-2 (KEK Report, 2005).

[4] P. Raimondi and A. Seryi, Phys. Rev. Lett. **86**, 3779 (2001).

[5] P. Bambade *et al.* (ATF Collaboration), Phys. Rev. ST Accel. Beams **13**, 042801 (2010).

[6] R. Apsimon, D. Bett, P. Burrows, G. Christian, B. Constance, M. Davis, A. Gerbershagen, C. Perry, and J. Resta-Lopez, Physics Procedia **37**, 2063 (2012), proceedings of the TIPP conference, 2011.

[7] G. White *et al.* (ATF2 Collaboration), Phys. Rev. Lett. **112**, 034802 (2014).

[8] R. Apsimon, D. Bett, N. Blaskovic Kraljevic, P. Burrows, G. Christian, C. Clarke, B. Constance, H. Dabiri Khah, M. Davis, C. Perry, J. Resta López, and C. Swinson, Phys. Rev. ST Accel. Beams **18**, 032803 (2015).

[9] A. Faus-Golfe, Private communication.

[10] `http://www.xilinx.com/support/documentation/data_sheets/ds100.pdf`.

[11] `http://www.ti.com/lit/ds/symlink/ads5474.pdf`.

[12] `http://www.analog.com/media/en/technical-documentation/data-sheets/AD9744.pdf`.

[13] `http://www.tmd.co.uk/`.

[14] CERN BE/ABP Accelerator Beam Physics Group, "MAD - Methodical Accelerator Design," `http://mad.web.cern.ch/mad/`.

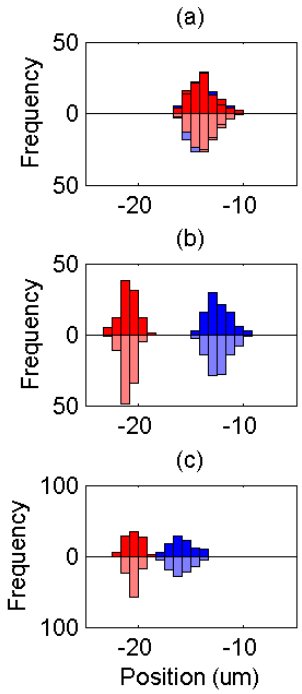

FIG. 10: Distributions of positions with feedback off (blue) and feedback on (red) at MQF15X for (a) the first, (b) the second, and (c) the third bunches. The darker, positive bars show the measured positions at MQF15X; the lighter, negative bars show the positions propagated to MQF15X. The mean position across all feedback off and on propagated data is adjusted to match that of the measured data, as the beam propagation does not take the absolute BPM position into account.

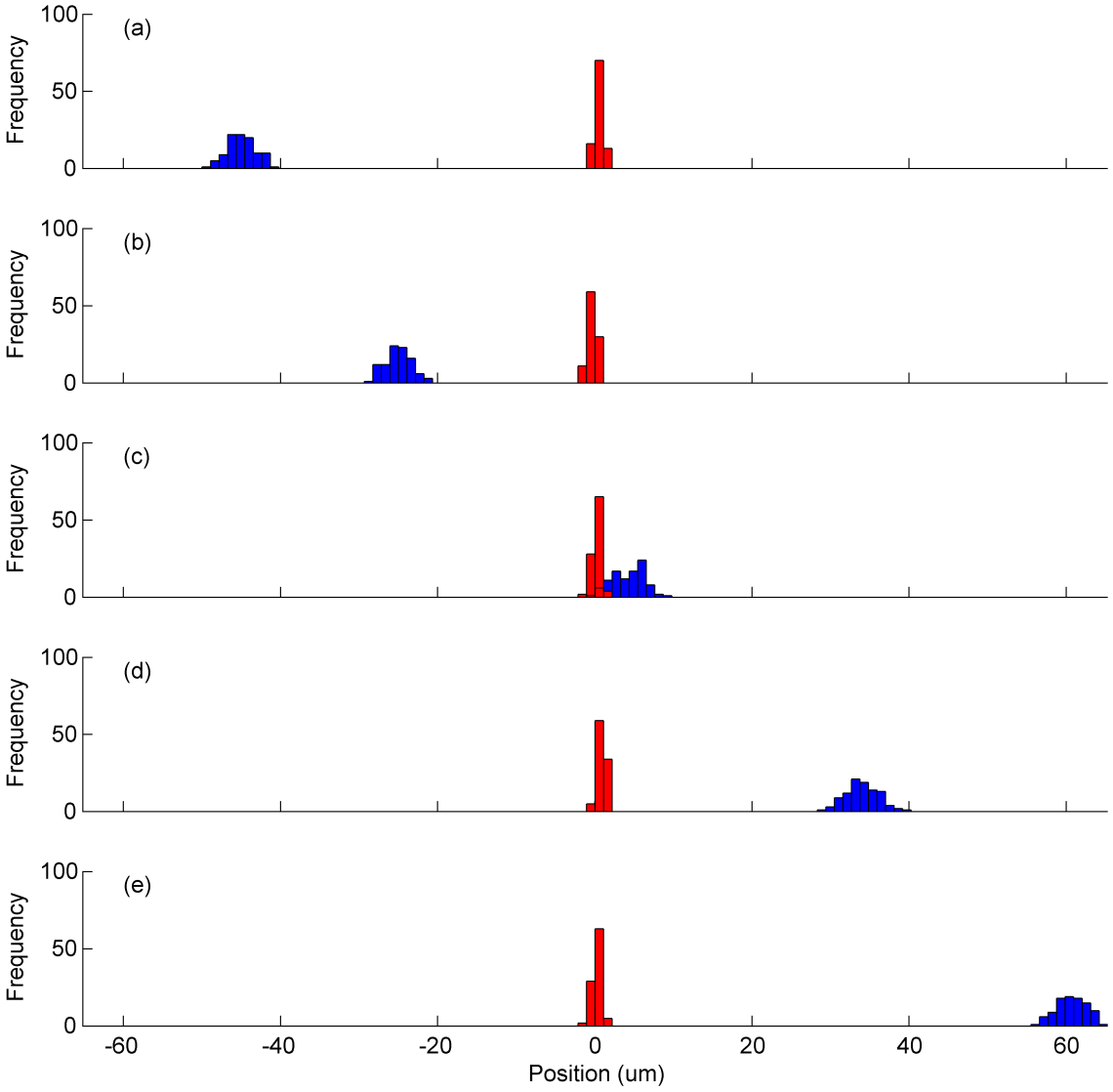

FIG. 11: Distributions of positions with feedback off (blue) and feedback on (red) for bunch 2 at P3 with a ZV6X current setting of (a) −0.292 A, (b) −0.298 A, (c) −0.304 A, (d) −0.310 A and (e) −0.316 A.

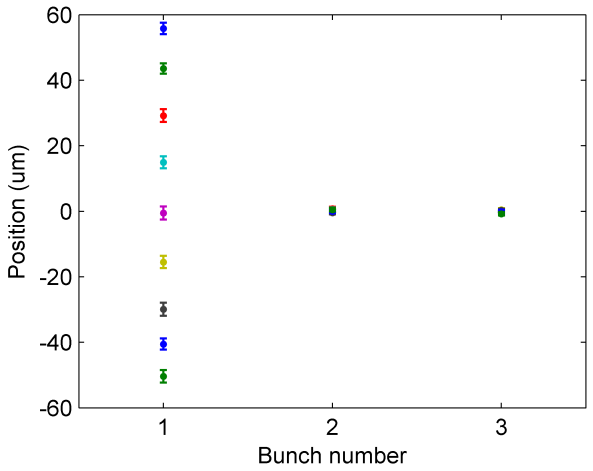

FIG. 12: Mean position measured at P3 with feedback on versus bunch number for nine incoming beam orbit settings (colour coded). Standard errors are given.

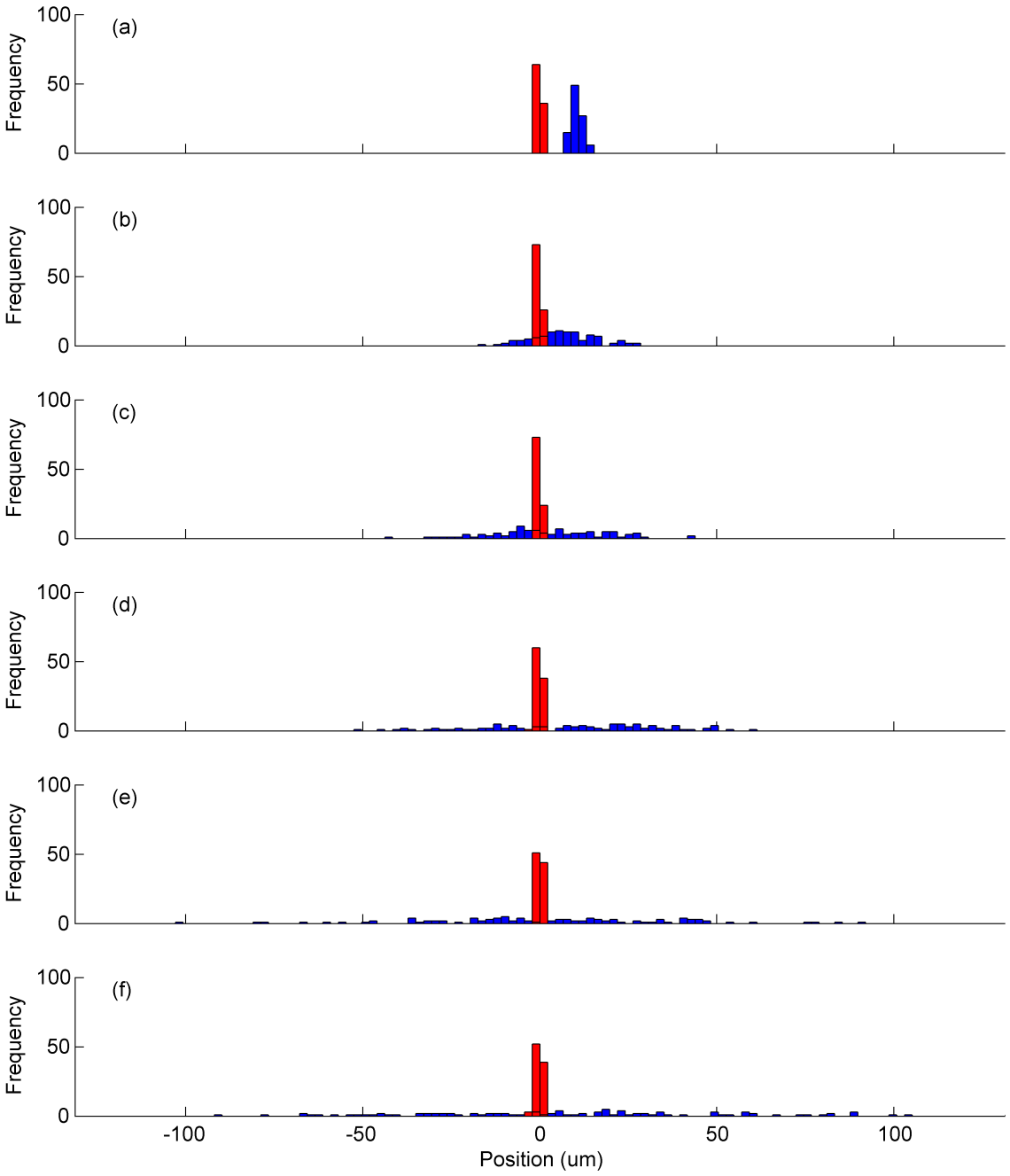

FIG. 13: Distributions of positions with feedback off (blue) and feedback on (red) for bunch 2 at P3 for a range of random jitter source strength settings.